

A comparative study between high-resolution imaging experiment and numerical simulation of a boiling bubble under subcooled convective flow

Hyunwoong Lee ^a, Hyungdae Kim ^{a*}, Guistini Giovanni ^b

^aDepartment of Nuclear Engineering, Kyung Hee University, Republic of Korea

^bDepartment of Mechanical, Aerospace and Civil Engineering, University of Manchester, United Kingdom

*Corresponding author: hdkims@khu.ac.kr

1. Introduction

Subcooled flow nucleate boiling is thermal-hydraulic phenomenon that occurs at a hot channel in a PWR (pressurized water reactor) and is directly related to the safety of reactor operation. [1] If a heat loads greater than the critical heat flux, which is a limit that can be removed by nuclear boiling heat transfer, DNB (Departure from Nucleate Boiling) occurs, nuclear fuel temperature rises rapidly and serious damage can occur. Various visualization experiments and computer simulation on subcooled flow nucleate boiling are being conducted to understand and accurately predict related physical phenomena to prevent accidents.

New simulation techniques are being investigated and developed to improve accuracy of CFD (Computational Fluid Dynamics). The recent rapid development of electronic and computer engineering technologies has reached the level of enabling Multi-phase CFD with Interface Tracking (M-CFD with IT) simulation, which describes boiling from the surface of nuclear fuel in the reactor by tracking the interface of individual bubbles in three dimensions. [2-3] Since high-resolution interface tracking CFD simulations show results sensitively reflected with artificially set interface tracking algorithm, it is desirable to verify accuracy using experimental data with similar resolution for the physical phenomenon of interest. [4]

However, when subcooled flow boiling is visualized using commonly used visible light sources, the difference in refractive index between liquid and vapor causes serious distortion of light at the interface. So, it is hard to obtain quantitatively reliable experimental data. In analysis using direct numerical simulation (DNS) and two-phase flow analysis using VOF interface tracking methods, small lattice sizes of 0.5 to 5 μm are essential for accurate flow prediction. Therefore, verification of interface tracking techniques based on the existing general flow visualization data can only determine the degree of qualitative similarity and there is a limit to the accuracy verification.

Our group tried to solve this problem with using synchrotron X-ray visualization with Pohang Light Source (PLS-II) at Pohang Accelerator laboratory (PAL). Fig. 1 shows a comparison of boiling visualization methods using X-ray and visible light. Visualization with X-ray can solve the problem of visible light due to parallel rays and small diffraction by wavelength. [5] As a result, we succeeded in obtaining high-resolution, high-frequency visualization results of subcooled flow boiling.

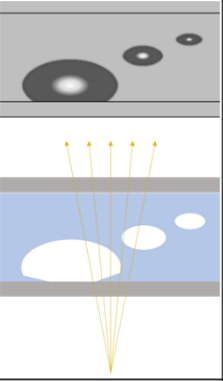
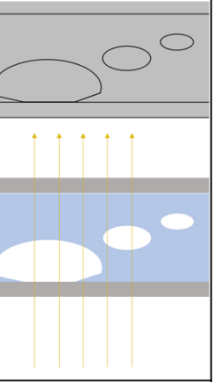
	Visible light	Synchrotron X-ray
Resolution	$\sim 10 \mu\text{m}$	$\sim 2 \mu\text{m}$
Distortion	O	X
Visualization		
Beam type	Scattered	Parallel

Fig. 1. Comparison with Visible light and X-ray

In this study, we use the X-ray visualization data obtained to verify M-CFD with IT simulation using OpenFOAM, which is open library CFD tool. We use the interMassTransFoam solver by adding the function of mass transfer and adjustment artificial interface thickness to InterFoam, the interface tracking-based multi-phase CFD solver. We simulated the subcooled flow nucleate boiling situation and optimized related simulation environment.

2. Experiment

In this section, experimental apparatus and setup with PAL-II are shortly described. Detailed descriptions of experimental methods and results have been dealt sensitively by previous studies. [5]

2.1 Experiment apparatus

A test section and an open flow loop were designed for optimizing experiments in the X-ray isolation room. The subcooled flow boiling experiment was conducted under 0.91 bar of pressure. Fig. 2 is schematic of experimental flow loop.

Degassed DI Water was used for working fluid. Water from the reservoir was pumped in a range of 26-104 $\text{kg/m}^2\text{s}$ of mass fluxes by a gear pump. Then, the pre-heater heated the water based on the temperature information of the thermocouple imbedded on the inlet of test section and set subcooling to 5-10 $^{\circ}\text{C}$. The water

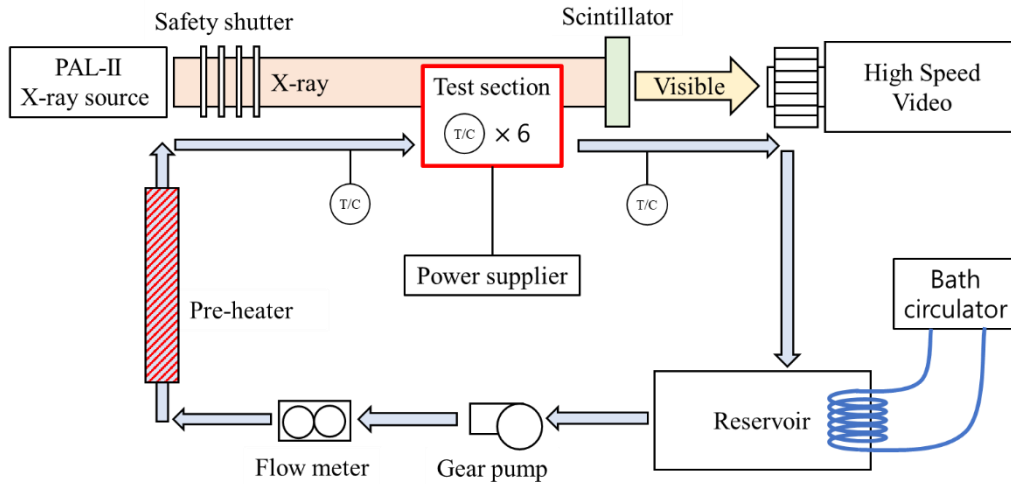


Fig. 2. Schematic of experimental flow loop

that has passed through the test section fell into the open reservoir. In the reservoir, the fluid is cooled to an appropriate level through an external bath circulator.

The test section receives heat through a cartridge heater connected to the power supplier. The supplied heat is applied directly to the bottom of the flow channel via a thin aluminum plate. Six thermocouples connected to this aluminum plate allow calculating the wall temperature and heat transfer amount to the channel. [5]

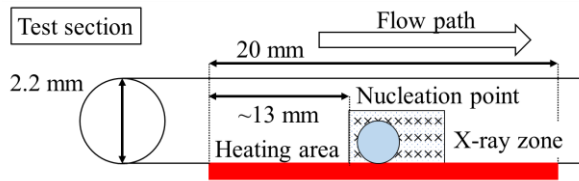


Fig. 3. Schematic of the flow channel in the test section

A circular channel of 2.2 mm diameter was perpendicularly irradiated through X-ray. Fig. 3 shows schematic of the flow channel in the test section. The heating area is 20mm. The camera used in the experiment was set by 1.1 μm of resolution and 2.2 mm \times 1.1 mm of field of view. This means that the nucleation point should be specified during observation.

2.2 Experimental results

For simulation, one specific bubble was selected in the various experiment results. Fig. 4 shows series of bubble growing observation with X-ray in the subcooled flow nucleate boiling. The value of each control variable with specific bubble is as follows.

Table I: Condition of the specific bubble growing

Subcooling	Applied heat flux	Nucleation site distance	Mass flux
9.7 K	190 kW/m ²	13 mm	90 kg/m ² s

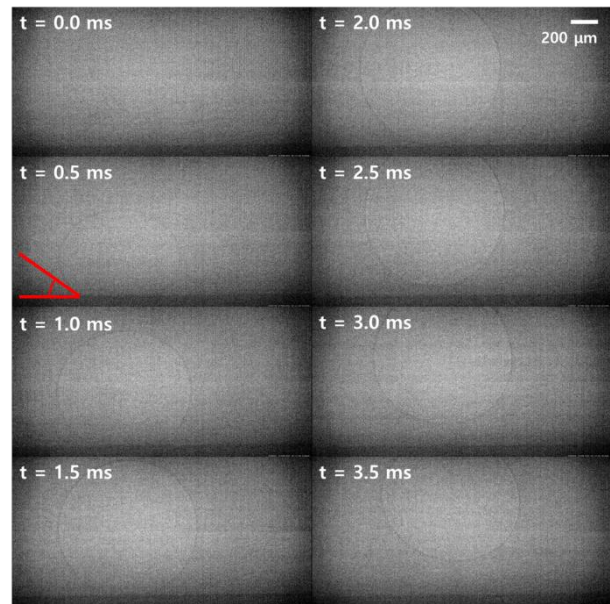


Fig. 4. Series of a bubble growing in subcooled flow boiling (9.7 K Subcooling, 190 kW Applied heat flux, 13mm distance with applied heat flux start point, 90 kg/m²s Mass flux)

3. Simulation

OpenFOAM, a CFD tool, was run to simulate the bubble growth results obtained through the experiment. Through collaborative research with the University of Manchester, the inhouse developed solver interMassTransFOAM was selected.

3.1 interMassTransFoam

InterMassTransFoam is an interFOAM-based solver capable of M-CFD with IT. This solver implements heat and mass transfer between each phase and is designed to incorporate the latest heat transfer variables into simulation such as interface thickness according to mesh size, thermal resistance at the interface, and thermal diffusion constant. [6]

3.2 Boundary condition and initial condition

Each variable measured in the experiment was set as the boundary condition of the simulation. It was run as a 2-dimension simulation with considering computational resources. In order to set boundary conditions on each wall, a $2.2 \text{ mm} \times 3.3 \text{ mm}$ geometry was built to cover all of the height directions of the channel. The mesh size was set to $2.0 \text{ }\mu\text{m}/\text{pixel}$ through the process of optimization. Along with this, the lower $100 \text{ }\mu\text{m}$ of geometry was divided meshing to have a finer resolution. Sensitivity test by mesh size was conducted. Additionally, condition of constantAlphaContactAngle was adopted to bottom surface. The value of the contact angle was tested by several condition.

A circle with a radius of $100 \text{ }\mu\text{m}$ was assumed to be an arbitrary bubble nucleation seed for initial condition. In addition, the channel flow without mass transfer was prerun to form the initial velocity boundary layer and thermal boundary layer before the bubble nucleates. Fig. 5 shows the appearance of the initial condition formed in this way.

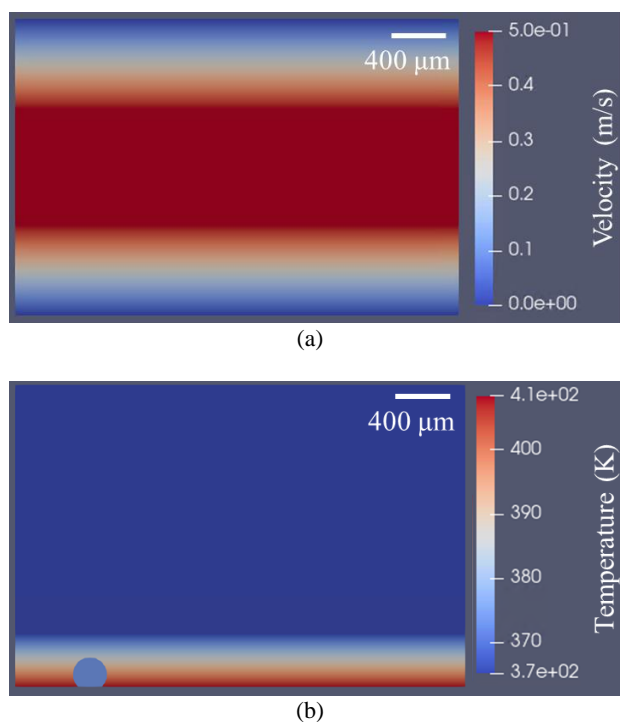


Fig.5. Initial condition of the simulation, (a) Velocity profile, (b) Temperature profile

4. Results

4.1 Contact angle sensitivity test

Sensitivity tests according to the change in the contact angle was conducted. Three values were used: 20° , experimentally observed value, 53° , which is the contact angle of general aluminum, and 70° , which is the contact angle of ITO. [7][8] The observed value was determined

using the angle between the floor surface and the bubbles based on Fig. 4, before the bubble departure (0.5 ms). Fig. 6 shows the results.

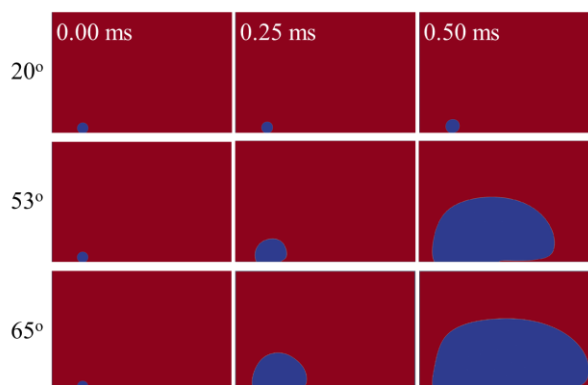


Fig. 6. Contact angle sensitivity test for 20° , 53° , and 65°

It can be observed that the growth tendency changes significantly according to the contact angle. The bigger the value, the faster it grew. It seems to require additional experiments on various surfaces to validate simulation results. But, nevertheless, bubble growth at 53° and 65° degrees is too much and out of touch with real phenomenon. For the validation of this simulation, 20° was selected that showed similar results to the experimental results.

4.2 Mesh size sensitivity test

Changes by mesh size were also tested. We compared the results for $2.0 \text{ }\mu\text{m}/\text{pixel}$ and $0.5 \text{ }\mu\text{m}/\text{pixel}$ for 20° degrees of contact angle. Fig. 7 shows the results.

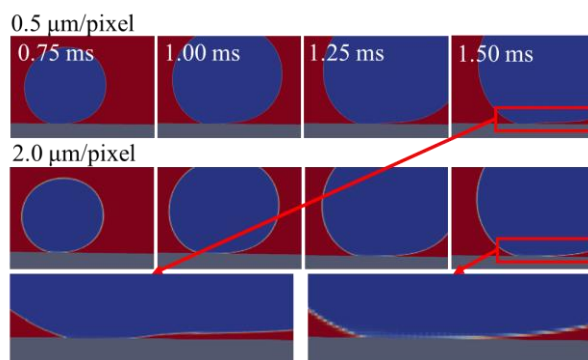


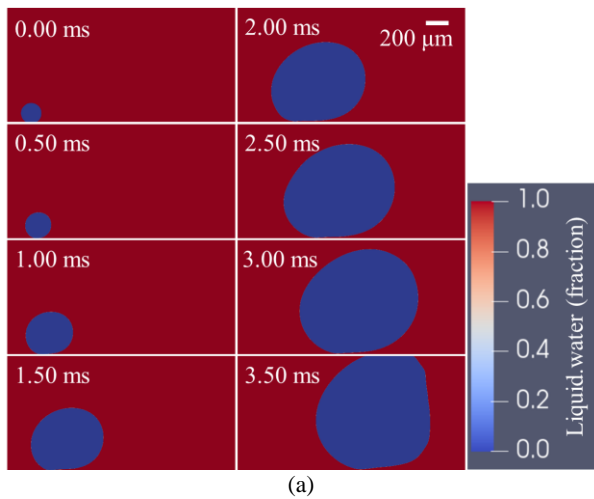
Fig. 7. Mesh size sensitivity test for 20° , 53° , and 65°

The growth of bubbles in the overall range did not change significantly. However, microlayer, the lower of bubble, is noteworthy. Generally, the value of the microlayer measured experimentally is under $10 \text{ }\mu\text{m}$. [9] The results of $2.0 \text{ }\mu\text{m}/\text{pixel}$, 5 pixels for microlayer, was insufficient to implement microlayers. There isn't observed the correct interface and the triple contact line, and the blur value is expressed compared to the fine mesh one.

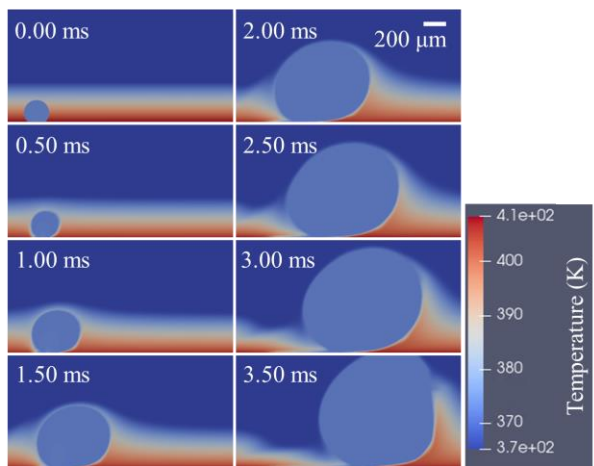
4.3 Comparison of simulation and experiment

The simulation results with temperature profile are shown in Fig. 8. It shows a general bubble growth tendency. When compared qualitatively with the experimental results in Fig. 4, it can be checked that the bubbles in the simulation are larger at the same time. It is expected that, in the experiment, the rapid growth of small bubbles could not be photographed through a proper exposure time, and the nucleation timing of bubble was incorrectly predicted in experiment.

In view of the temperature profile, it can be inferred that a strong heat transfer occurs because the temperature difference between the lower liquid part and the upper vapor part of the microlayer is very large. In addition, it was possible to observe the phenomenon in which the boundary layer was torn by the bubble.



(a)



(b)

Fig. 8. Visualized results of simulation: (a) Vapor fraction of water, (b) Temperature profile

Fig. 9 compares this result to experimental results by the bubble size in terms of quantitative aspects. The results at 0.5 ms observed in Fig. 4 were synchronized with the 1.5 ms result of the simulation according to the size of the bubble. Until 2.75 ms, these look similar.

However, after 3.0 ms, experimental data shows the bubble condensation, but simulation has not yet reached it.

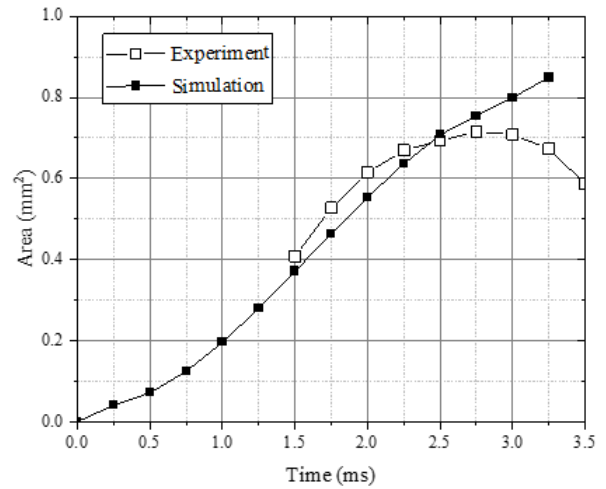


Fig. 9. Quantitative comparison with experiment and simulation

The bubble departure and dynamics can also be considered. From Fig. 4, Fig. 8 and Fig. 9, departure time of bubble was 2.75 ms in the experiment. However, in the simulation, even if it was 3.5 ms, it did not depart.

Overall, it can be inferred that the phase change in simulation is progressing slowly. This is expected to be due to a 2-dimensional simulation of the actual 3-dimensional situation. The phenomena like buoyancy and wall adhesion force, which appear differently on 2-dimension and 3-dimension, eventually retarded the bubble departure and slowed the bubble's growth.

5. Conclusion

For better prediction of heat transfer in the PWR system, CFD technology should be more detailed and validated. Using X-ray and M-CFD with IT, we viewed subcooled flow nucleate boiling as the μm scale on from various angles. The sensitivity test for contact angle and mesh size was conducted, and the reasonable factors were selected compared to the experimental results. As a result, we optimized several conditions of simulation and could observe various actions in actual phenomena through simulation. However, understanding of why these factors affect the overall trend is still lacking. For better comprehensions, more coordination of the geometry and various factors of the simulation and additional experiment will be needed.

ACKNOWLEDGEMENTS

This work was supported by the 'Global cooperative manpower education project for spent nuclear fuel management and advancement of innovative SMR design' of the Korea Institute of Energy Technology

Evaluation and Planning (KETEP) granted financial resource from the Ministry of Trade, Industry & Energy, Republic of Korea (No. 20214000000790)

REFERENCES

- [1] C.H.Lee, I. Mudawwar, A mechanistic critical heat flux model for subcooled flow boiling based on local bulk flow conditions, *International Journal of Multiphase Flow* 14(6), November 1988.
- [2] K.Ling, S.Zhang, W.Liu, X.Sui, W.Tao, Interface Tracking Simulation for Subcooled Flow Boiling Using VOSET Method, *Front. Energy Res.*, 22 January 2021.
- [3] V.K.Dhkir, G.R.Warrier, E.Aktinol, Numerical Simulation of Pool Boiling: A Review, *Journal of Heat Transfer* 135(6), June 2013.
- [4] Paek, K B, Cheon, S Y, Moon, S K, Yoon, Y J, and Park, J K. Visualization study of the subcooled flow boiling under various pressure condition. Korea, Republic of: N. p., 2004.
- [5] M. Kim, H. Lee, H. Kwak, D. Yu, H. Kim, Subcooled flow boiling visualization in mini channel using synchrotron X-ray: a preliminary test, *Transactions of the Korean Nuclear Society Spring Meeting*, May 18-20, 2022.
- [6] G. Giustini, R. I. Issa, A method for simulating interfacial mass transfer on arbitrary meshes, *Physics of Fluids* 33, 087102, 2021.
- [7] L. Carlos, G. Bartomeu, S. Bartolome, F. Antonio, R. Carmen, C. Antoni. Surface Modification of Pseudoboehmite-Coated Aluminum Plates with Squaramic Acid Amphiphiles. *ACS Omega*. 4. 2019.
- [8] H. Kim, M. Piao, S. Choi, C. Shin, Y. Lee, Development of Amperometric Hydrogen Peroxide Sensor Based on Horseradish Peroxidase-Immobilized Poly(Thiophene-co-EpoxyThiophene). *Sensors*. 8. 2008
- [9] S. Jung, H. Kim, Hydrodynamic formation of a microlayer underneath a boiling bubble, *International Journal of Heat and Mass Transfer* 120. 2018.